

Thermally cross-linkable hyperbranched polymers containing triphenylamine moieties: Synthesis, curing and application in light-emitting diodes

Juin-Meng Yu, Yun Chen*

Department of Chemical Engineering, National Cheng Kung University, Tainan 701, Taiwan

ARTICLE INFO

Article history:

Received 15 May 2010

Received in revised form

24 July 2010

Accepted 3 August 2010

Available online 7 August 2010

Keywords:

Hyperbranched polymers

Triphenylamine

Thermally cross-linkable

ABSTRACT

This paper demonstrates synthesis of hyperbranched polymers (**HTP** and **HTPOCH₃**), containing triphenylamine moieties in main chain and thermally cross-linkable periphery or terminal vinyl groups, and application as hole-transporting layer (HTL) in multilayer light-emitting diodes. Absorption and photoluminescence (PL) spectroscopy, cyclic voltammetry (CV) and differential scanning calorimetry (DSC) were employed to investigate their photophysical, electrochemical properties and thermal curing behaviors, respectively. The hyperbranched **HTP** and **HTPOCH₃** were readily cross-linked by heating scan, with the exothermic peaks being at 221 and 210 °C respectively. The glass-transition temperatures (T_g) of the hyperbranched polymers were higher than 140 °C after thermal cross-linking at 210 °C for 30 min. Multilayer light-emitting diodes (ITO/PEDOT:PSS/HTL/MEH-PPV/Ca/Al), using **HTP** and **HTPOCH₃** as HTL, were readily fabricated by successive spin-coating. The performance of MEH-PPV device (maximum luminance: 9310 cd/m², luminance efficiency: 0.26 cd/A) was effectively enhanced by inserting the thermally cross-linked **HTP** or **HTPOCH₃** as HTL (**HTP**: 12610 cd/m², 0.32 cd/A; **HTPOCH₃**: 14060 cd/m², 0.33 cd/A). This indicates that these thermally cross-linkable hyperbranched **HTP** and **HTPOCH₃** are very suitable for the fabrication of multilayer PLEDs using solution processes.

© 2010 Elsevier Ltd. All rights reserved.

1. Introduction

Hyperbranched polymers have gained much attention recently due to attractive advantages derived from their unique structures [1]. For example, hyperbranched structure has been introduced to conjugated polymers to suppress the formation of undesirable aggregate and excimer which generally deteriorates the performance of polymeric light-emitting diode (PLED) [2–6]. Hyperbranched polymers possess many advantages over linear counterparts, such as lower intrinsic viscosity, improved solubility and reduced intermolecular interaction [7]. Moreover, stable and homogeneous amorphous film is readily obtainable owing to reduced inter-chain cohesive force [8]. This amorphous and homogeneous morphology is critical for the fabrication of efficient multilayer light-emitting diodes [7–10]. Moreover, the terminal functional groups of a hyperbranched polymer can be readily changed by controlling the stoichiometry of feed monomers. For instance, the terminal of a hyperbranched polymers are reactive vinyl groups when prepared by the Heck coupling reaction using an excess of di- or trivinyl aromatic monomer [11–13]. Comparing to

linear counterparts, hyperbranched polymers possess higher concentration of reactive vinyl groups, leading to densely cross-linked structures after thermal curing. Highly cross-linked structures usually result in better solvent resistance and thermal stability. Solvent resistant characteristic is essential in the fabrication of multiple-layer polymeric light-emitting diodes (PLEDs), since it will prevent solvent erosion during subsequent spin-coating processes. Accordingly, solvent resistance is a prerequisite for hole-transporting polymers applied in PLEDs.

Polymeric light-emitting diodes have been viewed as major next-generation flat panel displays due to its low power consumption and large area display via spin-coating or inject-printing techniques [14–17]. To obtain high performance PLEDs necessitates efficient and balanced charges injection/transport from cathode and anode, respectively [18]. The multiple-layer EL devices are an alternative to attain efficient EL emission. But during the fabrication of a multiple-layer device the deposited layer may be dissolved by the subsequent spin-coating solution [19]. To avoid this undesirable dissolution, cross-linkable precursors with some specific functional groups become necessary for the device fabrication [18–21]. During EL device fabrication hole-transporting layer (HTL) is usually the first one deposited upon hole-injection PEDOT:PSS layer [22]. Triphenylamine-based derivatives are the most commonly used hole-transporting material due to their high hole mobility and

* Corresponding author. Tel.: +886 2085843; fax: +886 2344496.

E-mail address: yunchen@mail.ncku.edu.tw (Y. Chen).

ionization potential (high HOMO energy level). In general, high HOMO level is beneficial to hole-injection and transport [23,24]. Jen and coworkers synthesized numerous thermally cross-linkable hole-transporting materials derived from triphenylamine for solution processed polymer light-emitting diodes [18,25–28]. However, most polymer HTLs have been focused on linear structure with little attention paid to hyperbranched-based ones [29]. As mentioned above, the unique properties of hyperbranched polymers would result in EL devices with improved stability and efficiency over those of linear counterparts [24]. Reynolds and coworkers synthesized an AB₂-type monomer from triphenylamine, from which cross-linked hyperbranched polymer were obtained via the Heck reaction [24]. A PLED device using the hyperbranched polymer as HTL and MEH-PPV as emitting layer exhibited a maximum luminance of about 10⁴ cd/m².

We have successfully developed tri-functional fluorene derivatives to be applied in the preparation of hyperbranched copolyfluorenes [30–33]. As part of our effort in the preparation of hyperbranched copolyfluorenes for optoelectronic applications, we have further synthesized new thermally cross-linkable hyperbranched polymers from 2,4,7-trivinyl-9,9-dihexylfluorene (**3**) and triphenylamine-derived dibromo monomers (**4**, **5**) via the Heck reaction. The introduction of fluorene moiety into polymer main chain leads to not only good thermal and chemical stability but also good charge mobility [34–36]. Moreover, when applied as HTL in multilayer devices using MEH-PPV as emitting layer, the optoelectronic performances were greatly improved, with maximum luminance higher than 10⁴ cd/m². These results demonstrate that the hyperbranched polymers are promising hole-transporting materials for the fabrication of multilayer PLEDs.

2. Materials and methods

2.1. Materials and characterization

2,4,7-Tri(bromomethyl)-9,9-dihexylfluorene (**1**), 2,4,7-tri[methylene (triphenylphosphonium bromide)]-9,9-dihexylfluorene (**2**), 2,4,7-trivinyl-9,9-dihexylfluorene (**3**) and 4-methoxy-N,N-bis(4-bromophenyl)aniline (**5**) were synthesized according to the procedures reported previously [30,37]. The synthetic procedures and characterization data are described in the Supporting Information. Tri-*(o*-tolyl)phosphine, tributylamine and 4,4'-dibromotriphenylamine (**4**) were procured from Acros Co. and used as received. Palladium (II) acetate was purchased from Wako Co. and used without further purification. N,N-Dimethylformamide (DMF) and other reagents were used without further purification except specifically notified. All synthesized compounds were identified by ¹H NMR, ¹³C NMR, and elemental analysis (EA). The ¹H and ¹³C NMR spectra were recorded on a Bruker AMX-400 MHz FT-NMR, and the chemical shifts are reported in ppm using tetramethylsilane (TMS) as an internal standard. The molecular weights and molecular weight distributions of polymers were determined by a gel permeation chromatograph (GPC) using THF as eluent, using monodisperse polystyrene standards as calibration standards. The inherent viscosities were measured at concentration of 0.05 g dL⁻¹ in CHCl₃ at 30 °C using an Ubbelohde viscometer. The elemental analysis was carried out on a Heraeus CHN-Rapid elemental analyzer. The thermal curing behaviors and thermal transitional properties of the hyperbranched polymers were recorded using a differential scanning calorimeter (DSC), Mettler DSC 1, with a heating rate of 20 °C/min. Absorption and photoluminescence (PL) spectra were measured on a Jasco V-550 spectrophotometer and a Hitachi F-4500 spectrofluorometer, respectively. Electrochemical properties were investigated with a voltammetric analyzer (model CV-50W from Bioanalytical Systems, Inc.) equipped with a three-electrode cell. The cell was

made up of a polymer-coated glassy carbon as the working electrode, an Ag/AgCl electrode as the reference electrode, and a platinum wire as the auxiliary electrode. The electrodes were immersed in acetonitrile containing 0.1 M (*n*-Bu)₄NClO₄ as electrolyte. The energy levels were calculated using the ferrocene (FOC) value of -4.8 eV with respect to vacuum level, which is defined as zero [38]. Surface morphology and root-mean-square (rms) roughness of deposited polymer films were measured using an atomic force microscope (AFM) equipped with a Veeco/Digital Instrument Scanning Probe Microscope (tapping mode) and a Nanoscope IIIa controller. The root-mean-square (rms) roughness of a deposited polymer film was estimated by averaging the rms roughness of at least two different spots.

2.2. Synthesis of hyperbranched polymers (**HTP** and **HTPOCH₃**)

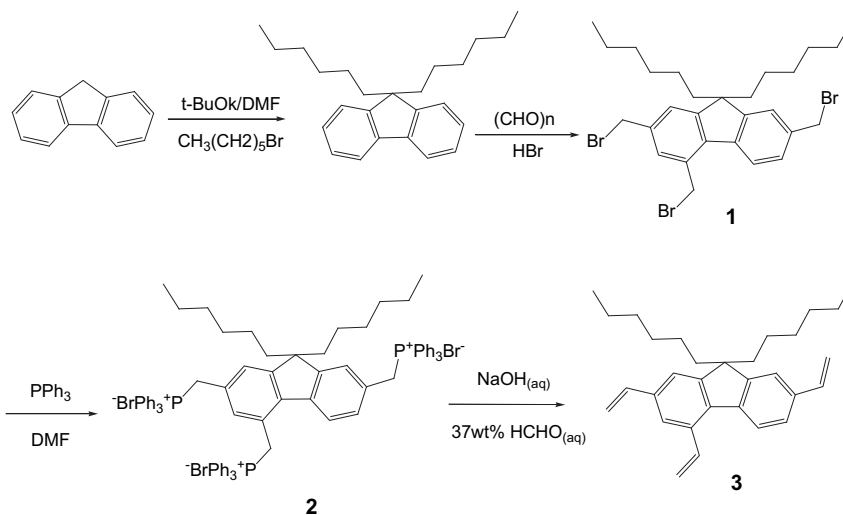
Hyperbranched polymers containing reactive vinyl groups were synthesized from dibromo compound (**4** or **5**) and an excess of trivinylfluorene (**3**) by the Heck coupling reaction. For example, a mixture of monomer **4** (0.12 g, 0.3 mmol), monomer **3** (0.13 g, 0.33 mmol), Pd(OAc)₂, tri-*o*-tolylphosphine, tributylamine, K₂CO₃, 7 mL of DMF, 10 mL of toluene and 0.5 mL of water was stirred at 100 °C for 46 min under nitrogen atmosphere. The solution was poured into a large amount of methanol and the appeared precipitate was collected by filtration and dried in vacuo at room temperature for 1 day to afford **HTP** (Yield: 56%). **HTPOCH₃** was prepared by analogous procedures, except using monomer **5** instead of monomer **4** (Yield: 45%).

HTP: ¹H NMR (400 MHz, CDCl₃, TMS, 25 °C): δ 7.81–7.03 (m, ArH), 6.84–6.76 (m, 2H, = CH-Ar), 5.83–5.78 (m, 3H, = CH₂), 5.50–5.48 (m, 1H, = CH₂), 5.29–5.25 (m, 2H, = CH₂), 1.99–1.95 (m, 4H, -CH₂-), 1.25–0.63 (m, 22H, -CH₂- and -CH₃). ¹³C NMR (400 MHz, CDCl₃, TMS, 25 °C): δ 152.1, 147.3, 146.9, 137.2, 135.7, 132.0, 129.3, 127.6, 127.3, 125.3, 124.7, 123.9, 123.3, 120.3, 119.4, 116.6, 54.3, 40.78, 31.4, 29.7, 23.6, 22.5, 13.9. Anal. Found (%) for **HTP**: C, 88.8; H, 7.9; N, 1.9.

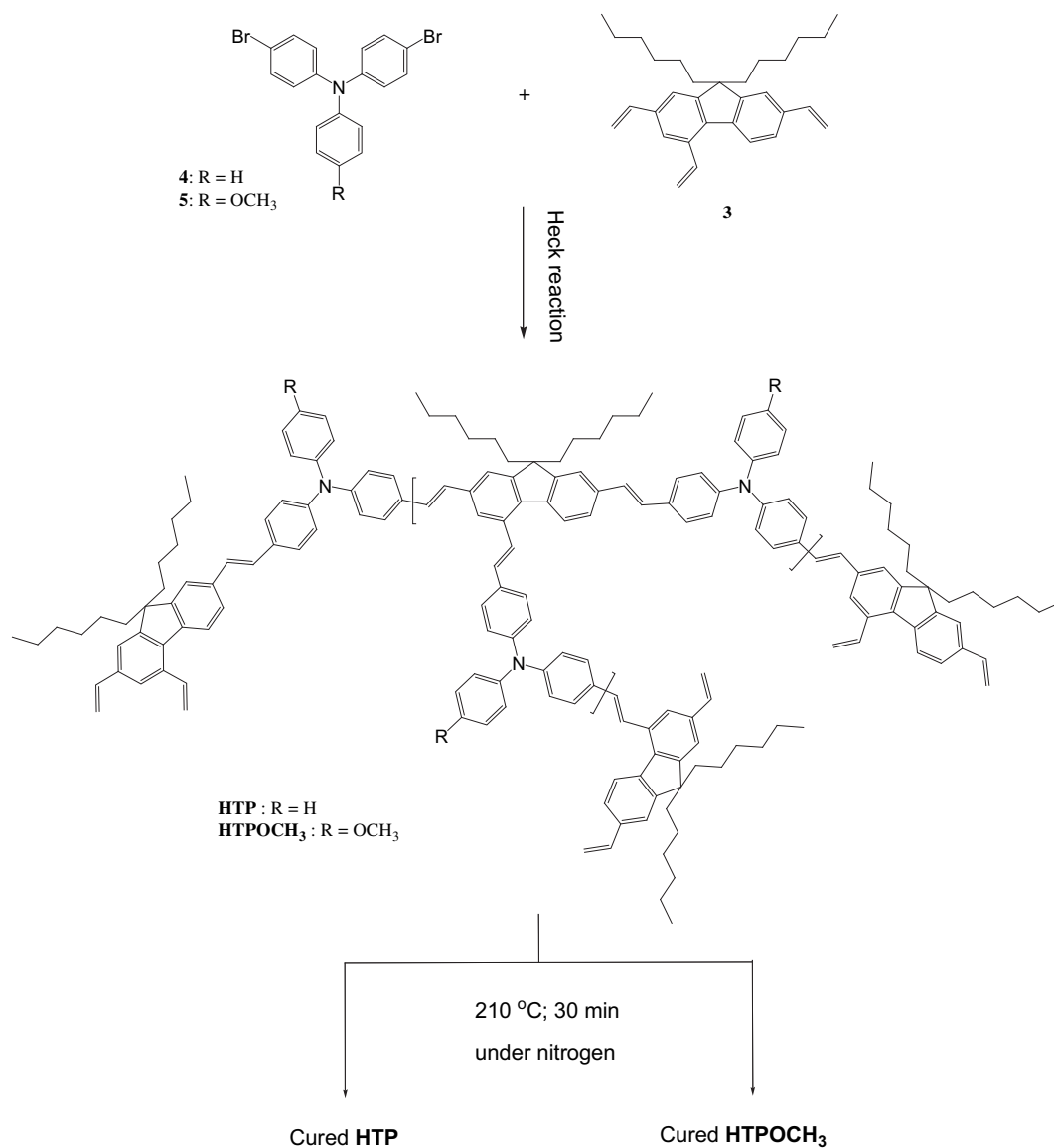
HTPOCH₃: ¹H NMR (400 MHz, CDCl₃, TMS, 25 °C): δ 7.79–7.01 (m, ArH), 6.87–6.81 (m, 2H, = CH-Ar), 5.83–5.78 (m, 3H, = CH₂), 5.50–5.48 (m, 1H, = CH₂), 5.29–5.21 (m, 2H, = CH₂), 3.83–3.78 (m, 3H, Ar-OCH₃), 1.99–1.95 (m, 4H, -CH₂-), 1.11–0.63 (m, 22H, -CH₂- and -CH₃). ¹³C NMR (400 MHz, CDCl₃, TMS, 25 °C): δ 156.5, 152.1, 147.2, 140.1, 137.2, 136.6, 135.7, 127.5, 127.2, 123.9, 123.3, 122.8, 120.2, 119.4, 116.6, 114.8, 55.5, 54.3, 40.7, 31.4, 29.7, 23.6, 22.5, 13.9. Anal. Found (%) for **HTPOCH₃**: C, 87.4; H, 8.0; N, 1.8.

2.3. Fabrication of light-emitting diodes

Multiple-layer light-emitting diodes (ITO/PEDOT:PSS/**HTP** or **HTPOCH₃**/MEH-PPV/Ca/Al) employing **HTP** or **HTPOCH₃** as hole-transporting layer were fabricated to investigate their optoelectronic characteristics. The device without the hole-transporting layer (ITO/PEDOT:PSS/MEH-PPV/Ca/Al) was also fabricated for comparative study. The ITO-coated substrate glasses were washed successively in ultrasonic baths of neutralizer reinerger/de-ionized water (1:3 v/v) mixture, de-ionized water, acetone and 2-propanol, followed with cleaning in a UV-ozone chamber. A thick hole-injection layer of PEDOT:PSS was spin-coated on top of the cleaned ITO glass and annealed at 150 °C for 15 min in a dust-free atmosphere. Upon the hole-injecting PEDOT:PSS layer was spin-coated (4000 rpm) with a hole-transporting layer from a hyperbranched polymer (**HTP** or **HTPOCH₃**) solution in chlorobenzene (1 mg/mL). The hole-transporting layer was cured at 210 °C for 30 min under nitrogen atmosphere; then it was spin-coated (3000 rpm) with MEH-PPV solution (10 mg/mL in chlorobenzene) to deposit emitting layer. Polymer solutions were filtered through a syringe



Scheme 1. Synthetic routes of branch monomer (**3**).



Scheme 2. Synthesis and thermal cross-linking of hyperbranched polymers (**HTP** and **HTPOCH₃**).

Table 1
Polymerization results and thermal properties of **HTP** and **HTPOCH₃**.

Polymer	M_n (10^4) ^a	M_w (10^4) ^a	PDI ^a	η_{inh}^b (dL/g)	ΔH (J/g) ^c	T_g (°C) ^c
HTP	0.7	1.5	2.1	0.82	42.9	109.2 (149.6)
HTPOCH₃	0.3	0.8	2.6	0.47	50.5	96.8 (141.7)

^a Determined by gel permeation chromatography using polystyrene as standard.

^b Inherent viscosity: measured at a concentration of 0.05 g/dL CHCl₃ at 30 °C.

^c Determined by differential scanning calorimeter (DSC) with a heating rate of 20 °C/min in the first heating scan. The values in the parentheses are the T_g s of the cured polymers (obtained from the second scan).

filter (0.2 μ m pore size) before the spin-coating. Finally, a thick layer of Ca and Al were successively deposited as cathode via vacuum deposition under 1×10^{-6} Torr. The luminance-bias, current density-bias, and EL spectral characteristics of the devices were recorded using a combination of Keithley power source (model 2400) and Ocean Optics usb2000 fluorescence spectrophotometer. Device fabrication was done in ambient conditions, with the following performance tests conducted in a glove-box filled with nitrogen.

3. Result and discussion

3.1. Synthesis and characterization of hyperbranched polymers (**HTP** and **HTPOCH₃**)

Dibromo monomer **5** was synthesized from 4-methoxy-N,N-diphenylaniline and N-bromosuccinimide, following the procedures reported in literature [37]. The preparation procedure of branch monomer 2,4,7-trivinyl-9,9-dihexylfluorene (**3**) had been reported in our previous study (Scheme 1) [30]. Hyperbranched hole-transporting polymers containing triphenylamine (**HTP** and **HTPOCH₃**) were synthesized via the Heck coupling reaction using $A_2 + BB'_2$ approach (Scheme 2). To increase the amount of reactive vinyl groups available for following thermal curing, an excess of monomer **3** was employed for the polymerization. However, the polymerization led to final gelation even at this stoichiometric imbalance due to the presence of tri-functional monomer **3**. In order to avoid the cross-linking of the polymers, the polymerization was interrupted before the gelation. This early interruption of polymerization gives rise to low polymer yields (45–56%). The

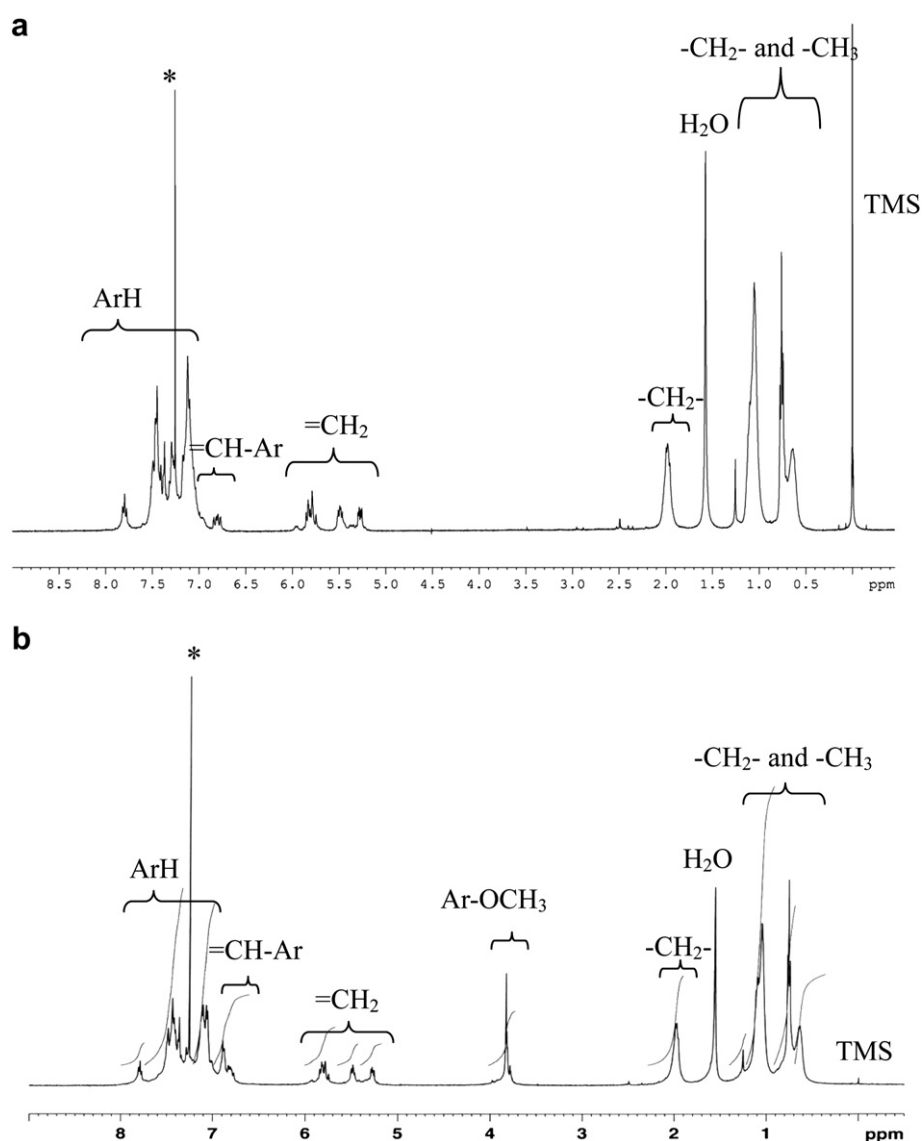


Fig. 1. ¹H NMR of **HTP** (a) and **HTPOCH₃** (b) dissolved in CDCl₃. The chemical shifts are reported in ppm using tetramethylsilane (TMS) as an internal standard (- refers to the signal caused by trace CHCl₃).

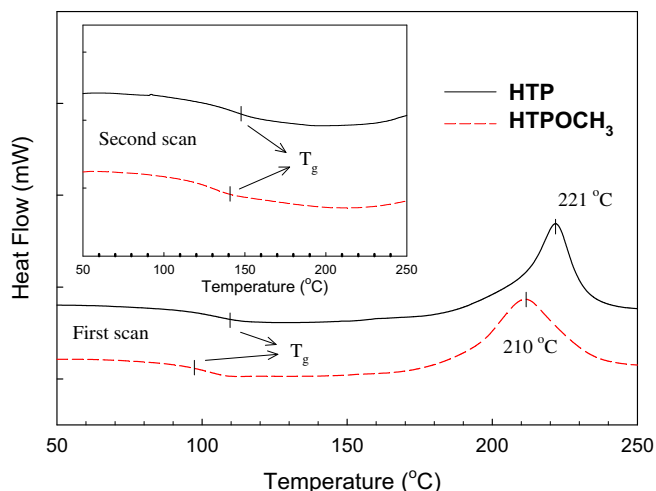


Fig. 2. DSC traces of **HTP** and **HTPOCH₃**. First run was used to observe the cross-linking reaction heat of vinyl groups. The second run was employed to examine completeness of the curing reaction and to determine the glass-transition temperature (inset). (Scan rate: 20 °C/min).

weight-average molecular weights (M_w) of **HTP** and **HTPOCH₃**, as determined by gel permeation chromatography using mono-disperse polystyrene as standard, was 1.5×10^4 and 0.8×10^4 (Table 1), with the polydispersity indexes (PDI) being 2.1 and 2.6, respectively. The large PDI values are attributable to growth rate difference between larger molecules and small ones. Because the growth rate is proportional to functionality, larger molecules grow faster than smaller ones that result in broadened molecular weight distribution [39]. The inherent viscosities of **HTP** and **HTPOCH₃**

measured in CHCl_3 (0.05 g/dL) at 30 °C were 0.82 and 0.47 dL/g, respectively, which were lower than that of linear poly(9,9-dihexylfluorene) (4.7 dL/g). The relative low inherent viscosities of **HTP** and **HTPOCH₃** support their branched structure [40]. The resulting polymers (**HTP** and **HTPOCH₃**) are readily soluble in common organic solvent such as chloroform and toluene. Fig. 1 shows the ^1H NMR spectra of the hyperbranched **HTP** and **HTPOCH₃**, in which the peaks located at 0.6–1.3 ppm and 2.0 ppm has been assigned to protons of pendant hexyl groups. The characteristic peaks at 5.2–6.0 ppm confirms the existence of periphery vinyl groups, from which thermally cross-linkable characteristic can be expected for the hyperbranched polymers.

3.2. Thermal curing and morphology study of the hyperbranched polymers

Since the hyperbranched polymers (**HTP**, **HTPOCH₃**) contain reactive vinyl groups in periphery and terminal units, they will form as three-dimensional structure by suitable thermal curing. The curing behaviors of the **HTP** and **HTPOCH₃** were investigated by differential scanning calorimetry (DSC) as shown in Fig. 2. During the first heating scan, the glass-transition temperatures (T_g) of the **HTP** and **HTPOCH₃** are observed at 109.2 °C and 96.8 °C, with exotherm peaks being at 221 °C and 210 °C, respectively. The exothermic heat is attributable to cross-linking reaction of the vinyl groups. After the first heating cycle, the glass-transition temperatures (T_g) of the **HTP** and **HTPOCH₃** are raised significantly to be 149.6 °C and 141.7 °C (inset), substantiating their thermal cross-linking reaction during the first scan. No obvious melting endothermic is observed in the DSC traces up to 250 °C. Accordingly, the hyperbranched polymers are basically amorphous materials with high T_g s, which can reduce the tendency of crystallization and

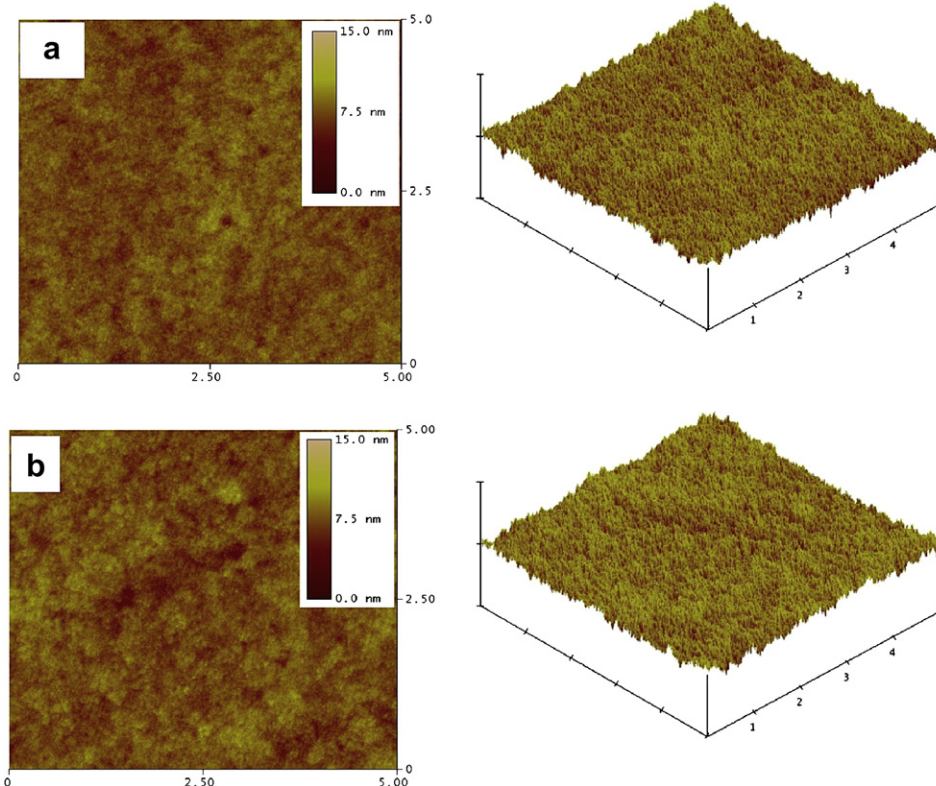


Fig. 3. The AFM images of (a) cured **HTP** and (b) cured **HTPOCH₃** films. The **HTP** and **HTPOCH₃** were coated on ITO glass and cured at 210 °C for 30 min under nitrogen atmosphere. (Scan size: $5 \times 5 \mu\text{m}$).

Table 2
Photophysical properties of **HTP** and **HTPOCH₃**.

Polymer	UV–vis λ_{\max} solution (nm) ^a	PL λ_{\max} solution (nm) ^a	UV–vis λ_{\max} film (nm)	PL λ_{\max} film (nm)
HTP	418, 341s ^b	478	424, 345s ^b	483
HTPOCH₃	423, 340s ^b	488	431, 344s ^b	494

^a 1×10^{-5} M in CHCl₃.^b The s means wavelength of shoulder.

maintain long-term morphological stability under device operation. To examine the appropriate curing time, their films were subjected to 210 °C to observe the exothermic behaviors for 80 min. As shown in the DSC traces (Fig. S1 in Supporting Information), the exothermic curing reaction is almost complete within 30 min. Therefore, the curing conditions of **HTP** and **HTPOCH₃** in the following investigations were set at 210 °C for 30 min under nitrogen atmosphere.

Successfully fabrication of PLED devices requires homogeneous and defect-free polymer layer to prevent reduced life-time and deteriorated performance. Volume shrinkage of prepolymers

during cross-linking often leads to microcrack formation in their cured products. This may also happen in the thermal curing of **HTP** and **HTPOCH₃** that increases undesirable surface roughness. Atomic force microscopy (AFM) was employed to observe their surface morphology and to estimate the root-mean-square (rms) roughness of pristine and cured polymer films. Fig. 3 shows the AFM images of cured **HTP** and **HTPOCH₃** films. Both **HTP** and **HTPOCH₃** exhibit homogeneous films after thermal curing at 210 °C for 30 min, no defect such crack or pinhole is observed in their AFM images. Moreover, the root-mean-square (rms) roughness of pristine **HTP** and **HTPOCH₃** films are 0.85 nm and 0.95 nm respectively. To fabricate efficient PLED device requires highly homogeneous film of each deposited polymers. Hyper-branched polymers can improve film morphology because of their highly branched and globular structure, which decreases the inter-chain cohesive force to result in more stable amorphous film [8–10,41]. Furthermore, the root-mean-square (rms) roughness of films can be decreased slightly to be 0.77 nm and 0.89 nm after the thermal curing. This means that the thermal curing raises not only solvent resistance but also smoothness of their film surface.

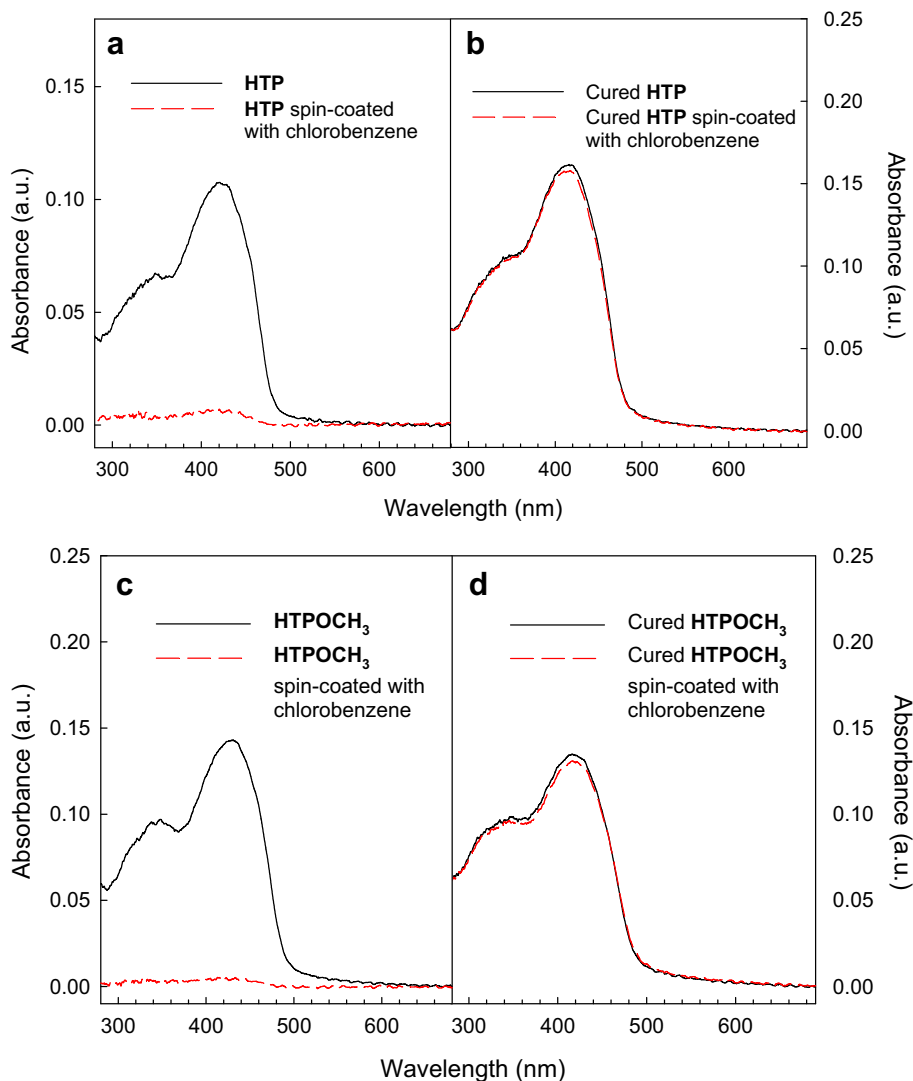


Fig. 4. Absorption spectra of **HTP** and **HTPOCH₃** before and after spin-coated with chlorobenzene: (a) and (c) are pristine films, (b) and (d) are thermally cured films (210 °C for 30 min under nitrogen atmosphere).

Table 3
Electrochemical properties of the **HTP** and **HTPOCH₃**.

	E_{ox} vs. FOC (V) ^a	E_{HOMO} (eV) ^b	E_{LUMO} (eV) ^c	$E_{\text{g}}^{\text{opt}}$ (eV) ^d
HTP	0.37(0.83)	-5.17	-2.60	2.57
HTPOCH₃	0.27(0.73)	-5.07	-2.44	2.53

^a $E_{\text{FOC}} = 0.46\text{V}$ vs. Ag/AgCl.

^b $E_{\text{HOMO}} = -e(E_{\text{ox, FOC}} + 4.8\text{ V})$.

^c $E_{\text{LUMO}} = -e(E_{\text{HOMO}} + E_{\text{g}}^{\text{opt}})$.

^d Band-gaps estimated from onset absorption (λ_{onset}): $E_{\text{g}}^{\text{opt}} = 1240/\lambda_{\text{onset}}$.

3.3. Photophysical properties of **HTP** and **HTPOCH₃**

Table 2 summarizes the characteristic optical data of **HTP** and **HTPOCH₃** in CHCl_3 and as thin films spin-coated on quartz plate, with their absorption and PL spectra being shown in Fig. S2 (Supporting Information). The **HTP** and **HTPOCH₃** in CHCl_3 show a absorption maxima at 418 nm and 423 nm with shoulders at 341 nm and 340 nm, which can be attributed to the $\pi-\pi^*$ transition of the main chain and the $n-\pi^*$ transition of the triphenylamine segments, respectively. In film state the absorption peaks red-shift slightly to 424 and 431 nm. The PL emission maxima in CHCl_3 locate at 478 and 488 nm for **HTP** and **HTPOCH₃** respectively, which shift bathochromically to 483 and 494 nm in film state. The red-shifts for **HTP** (5 nm) and **HTPOCH₃** (6 nm) in going from solution to film state are close to those of absorption (6 nm, 8 nm). This suggests that the undesirable inter-chain interactions are effectively prevented by the hyperbranched structures of the polymers.

Both **HTP** and **HTPOCH₃** are thermally cross-linkable polymers which are potentially applicable in the fabrication of multilayer PLED devices. However, highly solvent resistant is a prerequisite for multilayer PLEDs fabricated by solution processes. To examine the solvent resistance of the **HTP** and **HTPOCH₃** before and after thermal curing, a good solvent (chlorobenzene) was spin-coated on the top of the polymer films and then their absorption spectral variations were investigated. As shown in Fig. 4, the absorption spectra of the pristine **HTP** and **HTPOCH₃** films disappear almost completely after chlorobenzene spin-coating, indicating that the films are dissolved out during the coating process. However, the absorption spectral intensity of the thermally cured **HTP** and **HTPOCH₃** remains almost unchanged after the spin-coating. Their high solvent resistance is attributable to significantly increased cross-linking density after the thermal curing. The **HTP** and **HTPOCH₃** also reveal good resistant to toluene as shown in Fig. S3. The cured **HTP** and **HTPOCH₃** films are transparent films which are highly resistant toward organic solvent. Therefore, the solution-processable and thermally cross-linkable characteristics of **HTP** and

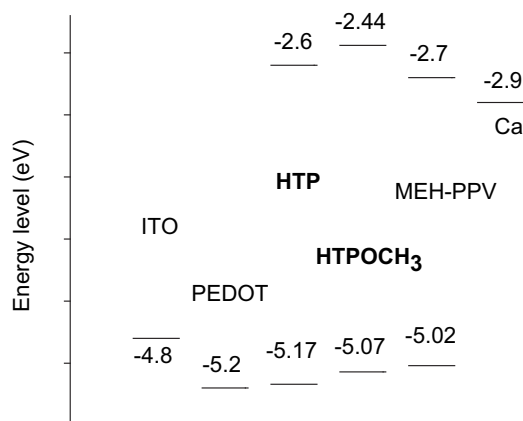


Fig. 5. The band diagrams of **HTP**, **HTPOCH₃**, PEDOT:PSS and electrodes.

Table 4
Optoelectronic properties of the light-emitting diodes^a.

Hole-transporting layer	Turn-on Voltage ^b (V)	Maximum Luminance (cd/m ²)	Luminance Efficiency (cd/A) ^c	CIE 1931 (x, y)
Non	3.1	9310	0.26	(0.55, 0.43)
HTP	2.7	12610	0.32	(0.56, 0.42)
HTPOCH₃	2.7	14060	0.33	(0.57, 0.42)

^a Device structure: ITO/PEDOT/Hole-transporting layer/MEH-PPV/Ca/Al.

^b Arbitrarily defined as the voltage required for a luminance of 10 cd/m².

^c The luminance efficiency at 1000 cd/m².

HTPOCH₃ are beneficial to the fabrication of multilayer PLED devices via inkjet-printing and other coating methods.

3.4. Electrochemical properties

Cyclic voltammetry (CV) has been constantly applied and considered as an effective tool to investigate electrochemical properties of conjugated polymers. **HTP**- or **HTPOCH₃**-coated ITO glasses were used as the working electrode, immersed in anhydrous acetonitrile containing 0.1 M tetra-*n*-butylammonium perchlorate (Bu_4NClO_4) as electrolyte, to conduct the CV measurements. Characteristic electrochemical data are summarized in Table 3. The highest occupied molecular orbital (HOMO) is estimated by using the equation $E_{\text{HOMO}} = -(E_{\text{ox}} + 4.8)\text{ eV}$, where E_{ox} is the onset oxidation potential relative to the ferrocene/ferrocenium couple.

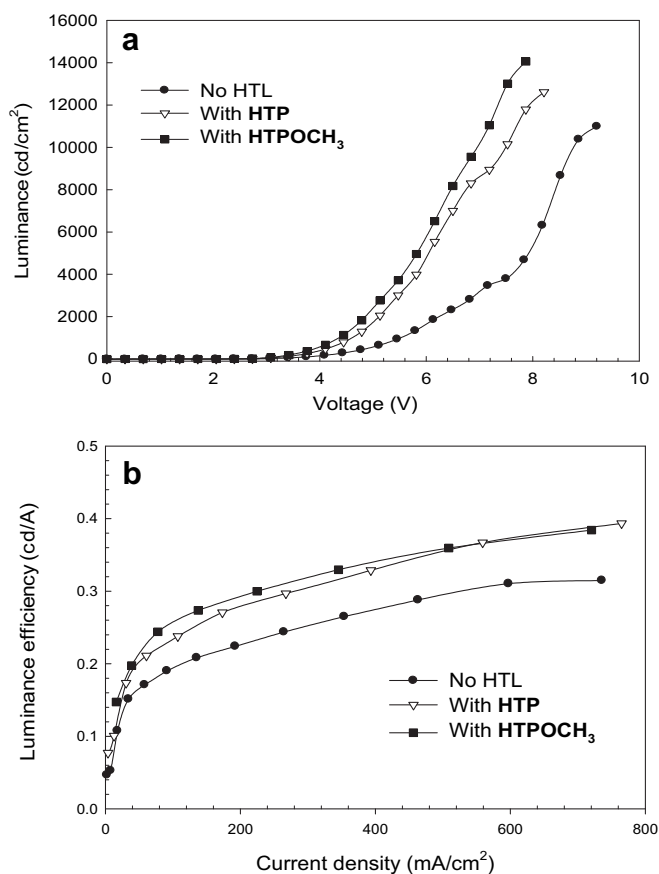


Fig. 6. (a) Brightness versus voltage and (b) luminance efficiency versus current density characteristics of multilayer PLEDs with or without hole-transporting **HTP** or **HTPOCH₃** layer. Device structure: ITO/PEDOT:PSS/(**HTP** or **HTPOCH₃**)/MEH-PPV/Ca/Al.

The lowest unoccupied molecular orbital (LUMO) is calculated by $E_{\text{LUMO}} = -e(E_{\text{HOMO}} + E_{\text{g}}^{\text{opt}})$, where the optical band-gap ($E_{\text{g}}^{\text{opt}}$) is estimated from onset absorption. The onset oxidation potentials of **HTP** and **HTPOCH₃** are 0.83 V and 0.73 V respectively. The much lower oxidation potential of **HTPOCH₃** is ascribed to the additional electron-donating methoxy groups at triphenylamine units. The HOMO level of **HTP** and **HTPOCH₃** are -5.17 and -5.07 eV and the LUMO levels are -2.6 and -2.44 eV respectively. The band diagrams of **HTP**, **HTPOCH₃**, PEDOT:PSS and work functions of electrodes are shown in Fig. 5. Clearly, the HOMO levels of **HTP** (-5.17 eV) and **HTPOCH₃** (-5.07 eV) are close to that of ITO/PEDOT:PSS (-5.2 eV), facilitating the injection and transport of holes. Accordingly, the hyperbranched polymers are potential hole-injection or hole-transporting materials.

3.5. Optoelectronic properties of light-emitting diodes using **HTP** and **HTPOCH₃** as hole-transporting layers

To demonstrate the application of the hyperbranched polymers (**HTP** and **HTPOCH₃**) as hole-transporting layer, multiple-layer PLEDs with a configuration of ITO/PEDOT:PSS/**HTP** or **HTPOCH₃**/MEH-PPV/Ca (50 nm)/Al (100 nm) were fabricated to investigate their optoelectronic characteristics. The hyperbranched polymers were spin-coated on top of ITO glass deposited with PEDOT:PSS, followed by thermal treatment at 210 °C for 30 min under nitrogen atmosphere to obtain transparent and insoluble films. The device without hole-transporting layer (ITO/PEDOT:PSS/MEH-PPV/Ca/Al) was also fabricated simultaneously for comparative study. Fig. 6 shows current density versus bias and luminance versus bias relationships of the EL devices, with the characteristic data summarized in Table 4. The main emission peaks are situated around 581 nm and 624 nm for all devices (Fig. 7), mainly contributed from MEH-PPV. Furthermore, the luminance efficiency (at 1000 cd/m²) and maximum luminance of MEH-PPV devices with **HTP** or **HTPOCH₃** as hole-transporting layer devices are superior to those without hole-transporting layer. For instance, the maximum luminance (luminance efficiency at 1000 cd/m²) of the devices are 12610 (0.32 cd/A) and 14060 cd/m² (0.33 cd/A) respectively, while it is 9310 cd/m² (0.26 cd/A) for that without hole-transporting layer. The luminance of **HTP**- or **HTPOCH₃**-based devices is improved when compared to the hyperbranched HTL reported by Reynolds [24]. The performance enhancement of the

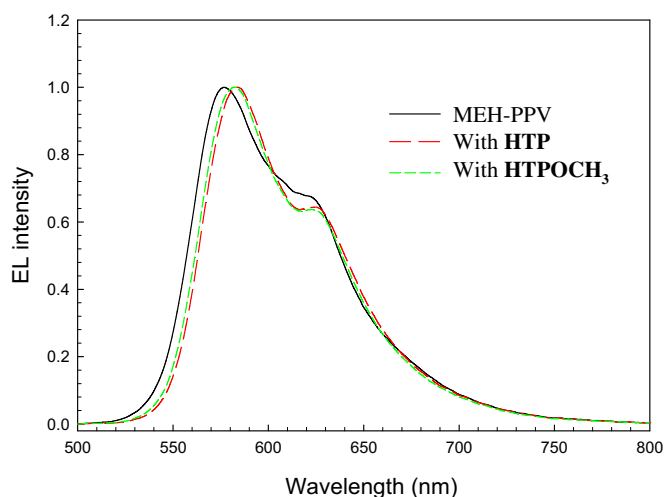


Fig. 7. EL spectra of multilayer device with or without thermally cured **HTP** or **HTPOCH₃** as hole-transporting layer. Device configuration: ITO/PEDOT:PSS/(hole-transporting layer)/MEH-PPV/Ca(50 nm)/Al(100 nm).

multilayer PLEDs seems contributed by a combination of several factors. Firstly, hole transport is facilitated due to high HOMO levels of the hyperbranched **HTP** (-5.17 eV) and **HTPOCH₃** (-5.07 eV). Secondly, the thermally cross-linked **HTP** or **HTPOCH₃** acts as a buffer layer not only to smooth surface but also to prevent PEDOT:PSS chain from penetrating into the emitting layer to quench the emission [18,42]. Finally, the hyperbranched **HTP** and **HTPOCH₃** also serve as electron-blocking layer, especially the latter, to increase the possibility of recombination in emitting layer (MEH-PPV). Consequently, **HTPOCH₃**-based device shows higher maximum luminance (14060 cd/m²) than **HTP**-based one (12610 cd/m²) due to its raised LUMO level. Furthermore, the energy levels of the hyperbranched polymers can be readily tuned by replacing the triphenylamine moieties with other hole-transporting groups. Accordingly, thermally cross-linkable hyperbranched polymers containing hole-transporting moieties are promising candidates for the fabrication of efficient multilayer PLEDs.

4. Conclusions

Two hyperbranched polymers (**HTP** and **HTPOCH₃**) containing triphenylamine moieties have been successfully synthesized via Heck reaction. The resulted hyperbranched polymers contain thermally reactive vinyl groups in periphery or terminal units. The hyperbranched **HTP** and **HTPOCH₃** were thermally cross-linked to form as transparent films. The **HTP** and **HTPOCH₃** demonstrated exothermic peaks at 221 °C and 210 °C, respectively, due to thermal cross-linking of the vinyl groups. The glass-transition temperatures (T_g) were 149.6 °C and 141.7 °C after thermal curing at 210 °C for 30 min. Moreover, both **HTP** and **HTPOCH₃** demonstrated homogeneous film morphology after thermal curing, with the root-mean-square (rms) roughness being 0.77 nm and 0.89 nm. The **HTP** and **HTPOCH₃** were used as HTL to fabricate multilayer light-emitting diodes (ITO/PEDOT:PSS/HTL/MEH-PPV/Ca/Al) by successive spin-coating process. The maximum luminances of the devices with HTL were 12610 and 14060 cd/m², with luminance efficiencies (at 1000 cd/m²) being 0.32 and 0.33 cd/A for **HTP** and **HTPOCH₃** respectively, which were superior to those of MEH-PPV device without HTL (9310 cd/m², 0.26 cd/A). Current results demonstrate that the thermally cross-linkable hyperbranched polymers are promising hole-transporting materials applicable for the fabrication of multilayer PLEDs. Furthermore, their hole-transporting ability can be readily adjusted by replacing triphenylamine moiety with other hole-transporting groups.

Acknowledgment

The authors thank the National Science Council of Taiwan for financial aid through project NSC 98-2221-E-006-003 MY3.

Appendix. Supplementary material

The supporting information associated with this article can be found in the on-line version at doi:10.1016/j.polymer.2010.08.001.

References

- [1] Lo S-C, Burn PL. Chem Rev 2007;107(4):1097–116.
- [2] He Q-Y, Lai W-Y, Ma Z, Chen D-Y, Huang W. Eur Polym J 2008;44(10):3169–76.
- [3] Tsai L-R, Chen Y. Macromolecules 2007;40(9):2984–92.
- [4] Tsai L-R, Chen Y. J Polym Sci Part A Polym Chem 2007;45(19):4465–76.
- [5] Tsai L-R, Lee C-W, Chen Y. J Polym Sci Part A Polym Chem 2008;46(17):5945–58.
- [6] Wu C-W, Lin H-C. Macromolecules 2006;39(21):7232–40.

- [7] Wang PW, Lin YJ, Devadoss C, Bharathi P, Moore JS. *Adv Mater* 1996;8(3):237–41.
- [8] Peng Q, Yan L, Chen D, Wang F, Wang P, Zou D. *J Polym Sci Part A Polym Chem* 2007;45(22):5296–307.
- [9] Wang H, Sun Y, Qi Z, Kong F, Ha Y, Yin S, et al. *Macromolecules* 2008;41(10):3537–42.
- [10] Wen G-A, Xin Y, Zhu X-R, Zeng W-J, Zhu R, Feng J-C, et al. *Polymer* 2007;48(7):1824–9.
- [11] Lim S-J, Seok DY, An B-K, Jung SD, Park SY. *Macromolecules* 2005;39(1):9–11.
- [12] Klarner G, Lee JI, Lee VY, Chan E, Chen JP, Nelson A, et al. *Chem Mater* 1999;11(7):1800–5.
- [13] Sun H, Liu Z, Hu Y, Wang L, Ma D, Jing X, et al. *J Polym Sci Part A Polym Chem* 2004;42(9):2124–9.
- [14] Burroughes JH, Bradley DDC, Brown AR, Marks RN, Mackay K, Friend RH, et al. *Nature* 1990;347(6293):539–41.
- [15] Akcelrud L. *Prog Polym Sci* 2003;28(6):875–962.
- [16] Hsiao C-C, Hsiao A-E, Chen S-A. *Adv Mater* 2008;20(10):1982–8.
- [17] Chen S-A, Lu H-H, Huang C-W. *Adv Polym Sci* 2008;49–84.
- [18] Huang F, Cheng Y-J, Zhang Y, Liu MS, Jen AKY. *J Mater Chem* 2008;18(38):4495–509.
- [19] Lin C-Y, Chen Y-M, Chen H-F, Fang F-C, Lin Y-C, Hung W-Y, et al. *Org Electron* 2009;10(1):181–8.
- [20] Park JH, Yun C, Park MH, Do Y, Yoo S, Lee MH. *Macromolecules* 2009;42(18):6840–3.
- [21] Lim B, Hwang J-T, Kim JY, Ghim J, Vak D, Noh Y-Y, et al. *Org Lett* 2006;8(21):4703–6.
- [22] Liu MS, Niu Y-H, Ka J-W, Yip H-L, Huang F, Luo J, et al. *Macromolecules* 2008;41(24):9570–80.
- [23] Shirota Y, Kageyama H. *Chem Rev* 2007;107(4):953–1010.
- [24] Paul GK, Mwaura J, Argun AA, Taraneekar P, Reynolds JR. *Macromolecules* 2006;39(23):7789–92.
- [25] Cheng Y-J, Liu MS, Zhang Y, Niu Y, Huang F, Ka J-W, et al. *Chem Mater* 2007;20(2):413–22.
- [26] Liu S, Jiang X, Ma H, Liu MS, Jen AKY. *Macromolecules* 2000;33(10):3514–7.
- [27] Shao Y, Gong X, Heeger AJ, Liu M, Jen AKY. *Adv Mater* 2009;21(19):1972–5.
- [28] Jiang XZ, Liu S, Liu MS, Herguth P, Jen AKY, Fong H, et al. *Adv Funct Mater* 2002;12(11–12):745–51.
- [29] Satoh N, Cho J-S, Higuchi M, Yamamoto K. *J Am Chem Soc* 2003;125(27):8104–5.
- [30] Yu J-M, Chen Y. *Macromolecules* 2009;42(21):8052–61.
- [31] Tsai L-R, Chen Y. *J Polym Sci Part A Polym Chem* 2007;45(23):5541–51.
- [32] Tsai L-R, Chen Y. *J Polym Sci Part A Polym Chem* 2008;46(1):70–84.
- [33] Tsai L-R, Chen Y. *Macromolecules* 2008;41(14):5098–106.
- [34] Redecker M, Bradley DDC, Inbasekaran M, Woo EP. *Appl Phys Lett* 1998;73(11):1565–7.
- [35] Babel A, Jenekhe SA. *Macromolecules* 2003;36(20):7759–64.
- [36] Redecker M, Bradley DDC, Inbasekaran M, Woo EP. *Appl Phys Lett* 1999;74(10):1400–2.
- [37] Tan Z, Tang R, Xi F, Li Y. *Polym Adv Technol* 2007;18(12):963–70.
- [38] Liu Y, Liu MS, Jen AKY. *Acta Polym* 1999;50(2–3):105–8.
- [39] Radke W, Litvinenko G, Müller AHE. *Macromolecules* 1998;31(2):239–48.
- [40] Gao C, Yan D. *Prog Polym Sci* 2004;29(3):183–275.
- [41] Robinson MR, Wang S, Bazan GC, Cao Y. *Adv Mater* 2000;12(22):1701–4.
- [42] Niu YH, Liu MS, Ka JW, Bardeker J, Zin MT, Schofield R, et al. *Adv Mater* 2007;19(2):300–4.